ELSEVIER

Coordination Chemistry Reviews
187 (1999) 233–254

COORDINATION CHEMISTRY REVIEWS

Energy surfaces, reorganization energies, and coupling elements in electron transfer☆

Bruce S. Brunschwig *, Norman Sutin [1]

Chemistry Department, Brookhaven National Laboratory, Upton, NY 11973-5000, USA

Received 27 July 1998; received in revised form 28 October 1998; accepted 11 November 1998

Contents

☆ Dedicated to Professor Ralph G. Pearson.

* Corresponding author. Fax: +1-516-344-5815.
E-mail address: bsb@bnl.gov (B.S. Brunschwig)
[1] Also corresponding author. Fax: +1-516-344-5815; e-mail: sutin@bnl.gov

PII: S0010-8545(98)00255-0

Abstract

The effects of changes in the shapes and intersections of the reactant and product free-energy surfaces on the vertical reorganization parameter and the free energy of activation for an electron self-exchange reaction are considered. Parabolic free energy surfaces provide a very good description of the inner-shell reorganization process even when the stretching force constants for the oxidized and reduced forms of the redox couple differ by a factor of two. The activation energy depends on the reorganization criterion and the contributions of the individual reactants to the inner-shell barrier are quite sensitive to the model used. Optical charge transfers and the consequences of reactant, product, and transition state stabilization in weakly interacting and very strongly interacting systems are also considered. Relationships between the equilibrium constant for the comproportionation reaction forming the mixed-valence complex and the optical charge transfer parameters are presented.

Keywords: Electron transfer; Energy surfaces; Reorganization energies; Electronic coupling elements

1. Introduction

The potential energies of the initial and final states of an electron transfer reaction (the reactants plus surrounding medium and the products plus surrounding medium) can be represented by multidimensional surfaces in nuclear configuration space [1–5]. These energy surfaces will have minima corresponding to the more stable nuclear configurations of the reactants and products and will intersect where the reactants and products have the same configurations and energies. In common with ordinary chemical reactions, an electron transfer reaction can then be described in terms of the motion of the system from the reactant minimum (initial state) to the product minimum (final state) on the lowest energy surface.

A detailed description of the electron transfer process can be obtained through the use of statistical mechanics [1,2]. Marcus showed that, provided a hypothetical change in charge on the reactants produces a proportional change in the dielectric polarization of the surrounding medium, the many-dimensional potential energy surface for the reactants and products can be reduced to harmonic free energy curves that are a function of a single reaction coordinate. Marcus further assumed that the free energy curves describing the distortions of the reactants and products from their equilibrium configurations also were harmonic with identical force constants [4].

The free energy of the close-contact reactants plus surrounding medium (Curve G_R) and the free energy of the close-contact products plus surrounding medium (Curve G_P) are plotted versus the reaction coordinate in Fig. 1 [3]. Electronic interaction of the redox orbitals of the reactants gives rise to the splitting of the energy curves (noncrossing) at their intersection. This splitting is equal to $2H_{ab}$, where H_{ab} is the electronic coupling matrix element. (We will treat H_{ab} as a positive quantity.) The minima of the noninteracting (zero-order or diabatic) parabolas are separated by $(2\lambda/f)^{1/2}$ where f is the reduced force constant for the parabolas and

λ, the reorganization parameter, is the vertical difference between the free energies of the noninteracting reactants and products at the reactants' equilibrium configuration for an electron transfer reaction with zero standard free energy change. Denoting the separation of the minima of the noninteracting reactant and product parabolas by a_o and the displacement along the reaction coordinate by x, a dimensionless reaction coordinate X may be defined as x/a_o: X varies from 0 to 1 as the reaction proceeds and is linearly related to the difference between the free energies of the reactants plus the surrounding medium (G_R) and the products plus the surrounding medium (G_P).

$$G_R = fx^2/2 = \lambda X^2 \tag{1a}$$

$$G_P = f(x - a_o)^2/2 + \Delta G^\circ = \lambda(X - 1)^2 + \Delta G^\circ \tag{1b}$$

$$(G_P - G_R) = (\lambda + \Delta G^\circ) - 2\lambda X \tag{1c}$$

At the transition state for the reaction, $G_R^* = G_P^*$ and $X^* = (\lambda + \Delta G^\circ)/2\lambda$ where ΔG°, the standard free energy change for the electron transfer, is negative for an exergonic reaction. Since $(G_P - G_R)$ and X are linearly related, the difference

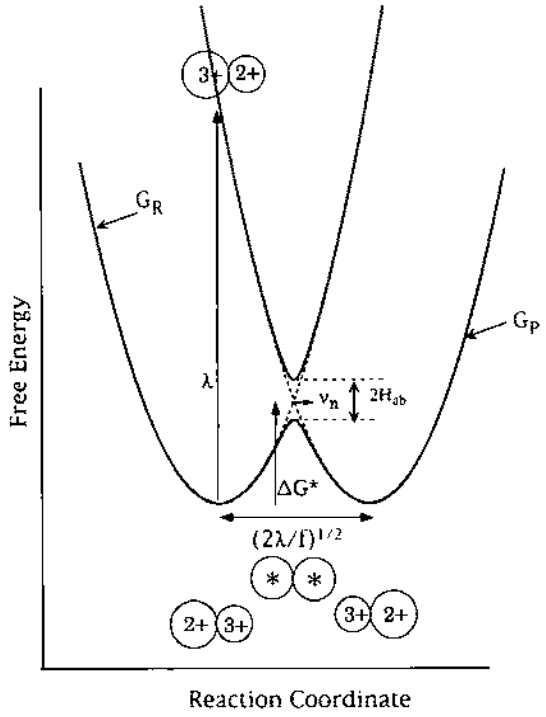

Fig. 1. Plot of the free energy of the close-contact reactants plus surrounding medium (G_R) and the free energy of the close-contact products plus surrounding medium (G_P) vs. the reaction coordinate for a self-exchange reaction ($\Delta G^\circ = 0$). Note that the reactant and product curves have identical force constants.

between the free energies of the reactants and products also affords a measure of the progress of the reaction [6,7].

The progress of the electron transfer reaction can also be described in terms of the mixing of the wave functions for the diabatic states. If ψ_a and ψ_b denote the wave functions of the zero-order initial (reactant) and final (product) states, their interaction gives rise to two linear combinations (the adiabatic states). The lower energy state, $\psi_g = c_a\psi_a + c_b\psi_b$, corresponds to the ground state and the upper, $\psi_e = c_a\psi_b - c_b\psi_a$, to the excited state when the overlap integral S_{ab} is neglected, (or is zero by construction [8]), and the mixing coefficients are normalized, i.e. $c_a^2 + c_b^2 = 1$. Since c_b^2, the square of the coefficient of the product wave function, equals the charge transferred to the electron acceptor, the value of c_b^2 also affords a measure of the progress of the reaction. Consequently c_b^2 also provides an alternative reaction coordinate [5].

In this article we discuss the relationship between the reorganization parameter and the free energy of activation for the electron transfer and examine the effect of changes in the shapes and intersections of the reactant and product curves on these energies. We also consider optical electron transfer and the consequences of reactant, product, and transition state stabilization in weakly interacting and strongly interacting systems. A number of common misconceptions are discussed.

2. Rate constant expressions

In terms of the classical treatment outlined above, the first-order rate constant for intramolecular electron transfer or for electron transfer within the precursor complex formed from the reactants in a bimolecular reaction is given by Eq. (2).

$$k_{el} = \kappa_{el}\nu_n \exp(-\Delta G^*/RT) \tag{2}$$

In this expression κ_{el} is the electronic transmission coefficient, ν_n is the nuclear vibration frequency that takes the system through the intersection region and ΔG^* is the free energy of activation for the electron transfer [5].

The electronic transmission coefficient is the probability that electron transfer will occur once the system has reached the intersection region (transition state). Provided that the electronic interaction of the reactants is sufficiently strong, $\kappa_{el} \approx 1$ and the electron transfer will occur with near unit probability in the intersection region: the electron transfer reaction is *adiabatic* with the system remaining on the lower energy surface on passing through the intersection region. Under these conditions k_{el} is given by

$$k_{el} = \nu_n \exp(-\Delta G^*/RT) \tag{3}$$

On the other hand, for a *nonadiabatic* reaction, $\kappa_{el} \ll 1$, $\kappa_{el}\nu_n = \nu_{el}$, and the rate constant is given by Eq. (4) where ν_{el} is the electron hopping frequency in the activated complex. The Landau–Zener treatment yields Eq. (5) for ν_{el} [9,10].

$$k_{el} = \nu_{el} \exp(-\Delta G^*/RT) \tag{4}$$

$$\nu_{el} = (2H_{ab}^2/h)(\pi^3/\lambda RT)^{1/2} \quad (5)$$

In effect, the adiabatic and nonadiabatic limits of the transition state formalism correspond to $\nu_{el} \gg \nu_n$ and $\nu_{el} \ll \nu_n$, respectively.

The free energy of activation for the electron transfer is given by

$$\Delta G^* = G_R^* - G_{min,R} \quad (6)$$

where G_R^* and $G_{min,R}$ are the free energies of the reactants at their transition state configuration and at their equilibrium configurations, respectively. The weakly interacting, intersecting parabola model leads to Eqs. (7a) and (7b) for ΔG^*.

$$\Delta G^* = \lambda(X^*)^2 \quad (7a)$$

$$= \lambda(1 + \Delta G°/\lambda)^2/4 \quad (7b)$$

The λ in these equations is the reorganization parameter introduced above. The free energy of activation for a self-exchange reaction ($\Delta G° = 0$) is equal to $\lambda/4$.

The reorganization parameter is usually broken down into inner-shell (vibrational) and outer-shell (solvational) components.

$$\lambda = \lambda_{in} + \lambda_{out} \quad (8)$$

The inner-shell reorganization energy depends upon the bond length changes and force constants of the reactants and products and is usually determined from the measured crystal or solution structures of the reactants and products and from their vibrational spectra. The distortions from the equilibrium configurations are generally treated within an harmonic approximation [11]. Although this approximation is usually adequate, it breaks down when the bond length changes are very large and it then becomes necessary to use a more elaborate force field. This is the case for the Cl_2/Cl_2^- couple. In favorable circumstances mode-specific reorganization energies can be obtained from resonance Raman intensity measurements [12]. The outer-shell reorganization energy depends upon the properties of the solvent. When a continuum model for the solvent is used, λ_{out} is a function of the dielectric properties of the medium, the distance separating the donor and acceptor sites, and the shape of the reactants. Various models for the solvent reorganization are available [13].

3. Inner-shell reorganization; diabatic expressions

In this section we consider the inner-shell reorganization parameter in greater detail and focus on the consequences of unequal reactant and product force constants.

3.1. Vertical reorganization energies and activation energies

As shown in Fig. 1, the reorganization parameter is the vertical difference between the (noninteracting) product and reactant free energies at the equilibrium

configuration of the reactants for a reaction with zero driving force. Since the parabolic curves in Fig. 1 have identical force constants, this energy difference is also equal to the difference between the reactant and product free energies at the equilibrium configuration of the products. In contrast, the activation energy is the difference between the free energies of the reactants (products) at their transition state configuration and at the reactants' equilibrium configuration (Eq. (6)). In order to illustrate the relation between vertical reorganization energies and activation energies we consider the symmetrical stretching vibrations of the reactants and products in the $Fe(H_2O)_6^{2+}$–$Fe(H_2O)_6^{3+}$ self-exchange reaction.

$$Fe(H_2O)_6^{2+} + Fe(H_2O)_6^{3+} = Fe(H_2O)_6^{3+} + Fe(H_2O)_6^{2+} \tag{9}$$

The inner-shell reorganization term is the sum of the reorganization parameters of the individual reactants, i.e.

$$\lambda_{in} = \lambda_2(d_2^0 \rightarrow d_3^0) + \lambda_3(d_3^0 \rightarrow d_2^0) \tag{10}$$

The first term on the right hand side is the energy required to change the Fe–O distance in $Fe(H_2O)_6^{2+}$ from its equilibrium value d_2^0 to the equilibrium value d_3^0 in $Fe(H_2O)_6^{3+}$, and the second term is the energy required to change the Fe–O distance in $Fe(H_2O)_6^{3+}$ from d_3^0 to d_2^0. Denoting $(d_2^0 - d_3^0)$ by Δd^0, the vertical reorganization energy is given by Eqs. (11a) and (11b):

$$\lambda_{in} = 6f_2(\Delta d^0)^2/2 + 6f_3(\Delta d^0)^2/2 \tag{11a}$$

$$= 3(f_2 + f_3)(\Delta d^0)^2 \tag{11b}$$

Further, λ_2/λ_3, the ratio of the contributions of the individual reactants to the vertical reorganization energy, is equal to f_2/f_3. Evidently the contributions of the $Fe(H_2O)_6^{2+}$ and $Fe(H_2O)_6^{3+}$ breathing modes to λ_{in} are *directly* proportional to their respective force constants.

Considering the activation process, energy conservation requires that the Fe–O distances in the two reactants adjust to a common value (transition-state configuration) where $G_R = G_P$ prior to the electron transfer. We denote this common distance by d^*. The energy required to reorganize the two reactants to the transition-state configuration is then

$$\Delta G_{in}^* = 3f_2(d_2^0 - d^*)^2 + 3f_3(d^* - d_3^0)^2 \tag{12}$$

Minimizing the activation energy yields Eq. (13) and substitution into Eq. (12) gives Eqs. (14a) and (14b).

$$d^* = \frac{f_2 d_2^0 + f_3 d_3^0}{f_2 + f_3} \tag{13}$$

$$\Delta G_{in}^* = \frac{3f_2 f_3 (\Delta d^0)^2}{f_2 + f_3} \tag{14a}$$

$$= \frac{\lambda_2 \lambda_3}{\lambda_2 + \lambda_3} \tag{14b}$$

Since their breathing force constants differ, the activation energies for reorganizing the $Fe(H_2O)_6^{2+}$ and $Fe(H_2O)_6^{3+}$ ions are not equal. Substitution of d^* into Eq. (12) and taking the ratio of the individual reorganization energies gives

$$\frac{\Delta G_{in}^*(Fe(H_2O)_6^{2+})}{\Delta G_{in}^*(Fe(H_2O)_6^{3+})} = \frac{f_3}{f_2} \tag{15}$$

In contrast to their contributions to λ_{in}, the ratio of the contributions of $Fe(H_2O)_6^{2+}$ and $Fe(H_2O)_6^{3+}$ to ΔG_{in}^* are seen to be *inversely* proportional to their force constants. Since f_3 is larger than f_2, the $Fe(H_2O)_6^{2+}$ ion reorganizes more than the $Fe(H_2O)_6^{3+}$ ion. Moreover, $\Delta G_{in}^* < \lambda_{in}/4$, i.e. the activation energy is less than one-quarter the reorganization term! The breakdown in the often used $\Delta G_{in}^* = \lambda_{in}/4$ relation arises because the free energy surfaces are not, in general, harmonic along the reaction coordinate. A measure of the anharmonicity is provided by the fractional difference between one-quarter of the reorganization term and the activation energy (Eq. (16)).

$$\frac{\lambda_{in}/4 - \Delta G_{in}^*}{\Delta G_{in}^*} = \frac{(f_2 - f_3)^2}{4f_2f_3} \tag{16}$$

For the $Fe(H_2O)_6^{2+}$–$Fe(H_2O)_6^{3+}$ self-exchange the difference amounts to about 5% [10].

Considerable simplification results from constructing energy surfaces using a common, reduced value f_{in} for the force constant of the $Fe(H_2O)_6^{2+}$ and $Fe(H_2O)_6^{3+}$ symmetrical stretching vibrations.

$$f_{in} = \frac{2f_2f_3}{(f_2 + f_3)} \tag{17}$$

Under these conditions

$$d_{rf}^* = (d_2^0 + d_3^0)/2 \tag{18a}$$

$$\lambda_{rf} = 6f_{in}(\Delta d^0)^2 \tag{18b}$$

$$\Delta G_{rf}^* = \Delta G_{in}^* = 3f_{in}(\Delta d^0)^2/2 = \lambda_{rf}/4 \tag{18c}$$

and the two reactants reorganize to the same extent with ΔG_{rf}^* now equal to $\lambda_{rf}/4$. Note that replacing f_2 and f_3 by f_{in} does not change the value of the activation energy (i.e. $\Delta G_{rf}^* = \Delta G_{in}^*$, Eq. (14a)) but does change the value of λ (Eqs. (11b) and (18b)).

Horizontal sections through the energy wells defined by the stretching vibrations of the reactants and products are presented in Fig. 2. The well in the upper left of the figure describes the energy of the reactants as a function of their nuclear configurations while the well in the lower right shows the energy of the products as a function of their configurations. The dashed line is the reaction coordinate, generated by plotting the projection of the (minimum energy) intersection of the surfaces on the xy plane as the product minimum is displaced vertically. An alternative, more rigorous, definition of the reaction coordinate has been given by Warshell [6,7]. Warshell defines the reaction coordinate Q as equal to the potential

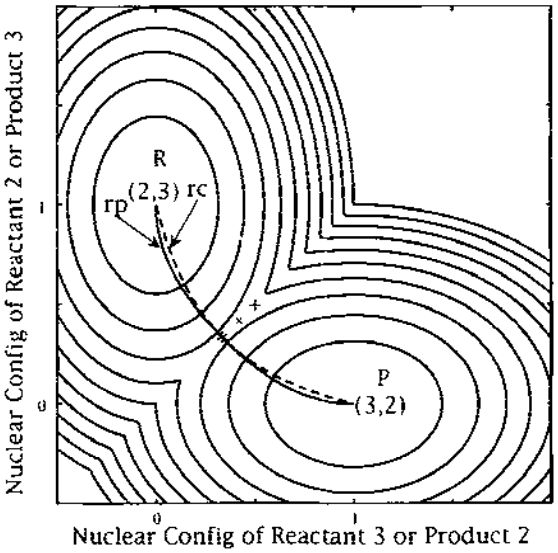

Fig. 2. Contour plots of the free energy of the close-contact reactants (and products) plus surrounding medium vs. a nuclear coordinate of reactant 2, R_2, (product 3, P_3) and a nuclear coordinate of reactant 3, R_3, (product 2, P_2,) for a self-exchange reaction ($\Delta G^\circ = 0$). In most cases of electron transfer between symmetrical metal complexes the nuclear coordinate for the inner-shell reorganization will correspond to a normal coordinate associated with the harmonic stretch of the metal-ligand bonds. The reaction path (solid line, rp) and the reaction coordinate (dashed line, rc) are also shown. The symbols *, x, and + indicate the positions of the transition state, the crossing point, and the midpoint, respectively, for the free energy curves shown in Fig. 4.

energy difference between the precursor complex (the reactants plus their surrounding medium) and the successor complex. All configurations with the same potential energy difference have the same value of Q. The free energy function at a given value of Q is determined from the number of configurations of the system that correspond to the particular potential energy difference, $G_R(Q) = -RT \ln(p(Q)_R)$, where $p(Q)_R$ is the probability that the system will have a given value of Q. The reaction coordinate defined in this manner is closely related to the reaction coordinate X defined in Section 1 and the dashed line in Fig. 2 also shows the configurations that contribute most to the free energy function. The solid line in Fig. 2 is the reaction path, defined as the path of steepest decent from the intersection (activated complex) to the reactants' and products' energy minima. Since the surfaces in Fig. 2 are not harmonic along the reaction coordinate, a plot of the free energy along the reaction coordinate does not yield the parabolic energy curves shown in Fig. 1. However, use of reduced force constants yields energy wells with circular cross-sections and results in the curves shown in Fig. 1. The difference between the energies along the reaction coordinate and the reaction path is illustrated in Fig. 3 for the surfaces shown in Fig. 2.

3.2. Individual reactant reorganization energies

We have seen that when the symmetrical breathing modes of the reactants and products of a self-exchange reaction are considered, the activation energy for the inner-shell reorganization is given by Eqs. (14a) and (14b). Further, when the breathing modes for the oxidized and reduced forms of a couple have different force constants, the two reactants in a self-exchange reaction reorganize to different extents. Within the Marcus framework the activation energy is obtained by locating the minimum on the 'line' where $G_R = G_P$. Another way of describing the reorganization process is through the use of separate free-energy curves for the individual reactants and products. For a self-exchange reaction the two redox pairs are the same so that only a single pair of energy curves is needed [14]. Since we only consider distortions of the reactants and products from their equilibrium configurations, the minima of the energy curves for the redox partners are drawn at the same energy. The individual curves are shown in Fig. 4. The activation energy is the sum $\Delta G_2^* + \Delta G_3^*$. Note that the transition state configuration, d^*, does not occur at the intersection of the individual energy curves. In this section we consider the effect of different assumptions for the reorganization condition that are sometimes made.

3.2.1. The reactants reorganize to the midpoint defined by $d_{mp} = (d_2^0 + d_3^0)/2$ (cf. Eq. (18a))

The inner-shell reorganization energy required to reach this configuration is given by Eq. (19).

$$\Delta G_{mp} = 3(f_2 + f_3)(\Delta d^0/2)^2 \tag{19}$$

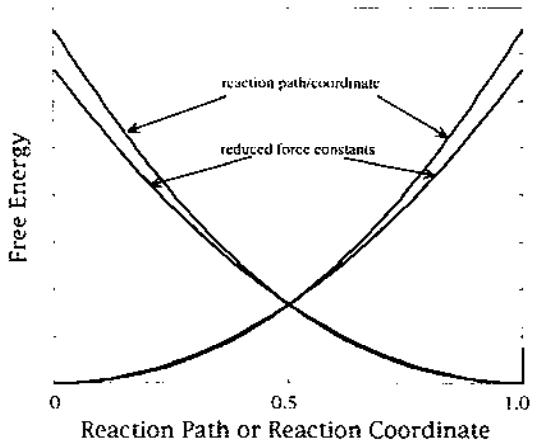

Fig. 3. Plot of the free energy of the reactants and products along the reaction path and the reaction coordinate vs. the reaction path and/or reaction coordinate normalized to unit length. Also shown is the free energy of the reactants and products calculated with reduced force constants, corresponding to the traditional Marcus energy surfaces. In the latter description the straight line connecting the reactant and product minima constitutes both the reaction path and the reaction coordinate.

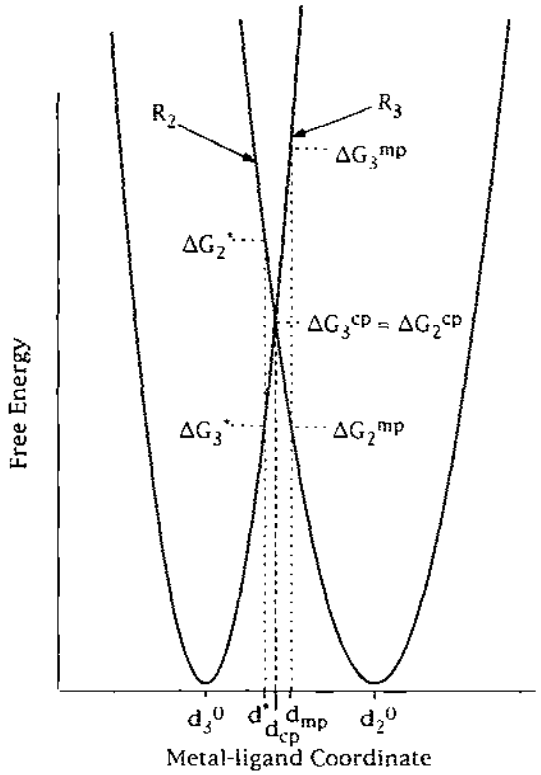

Fig. 4. Plot of the free energies of the individual reactants (R_2 and R_3) vs. their metal-ligand coordinate. R_3 is shown on the left and R_2 is shown on the right. The energy minima of the curves are assumed equal and the reactant energies required to attain the transition state, the crossing point, and the midpoint configurations are shown.

The vertical energy difference does not change and ΔG_{mp} is equal to $\lambda_{in}/4$. It can readily be seen that $\Delta G^{*}_{in} < \Delta G_{mp}$. Note that the contribution of each reactant to the energy at the midpoint configuration is proportional to its stretching force constant. This is inverse to its contribution to the transition state energy (Eq. (15)).

3.2.2. The reactants reorganize to the intersection of the individual reactant parabolas where d at the crossing point is given by Eq. (20)

$$d_{cp} = \frac{\sqrt{f_2}d_2^0 + \sqrt{f_3}d_3^0}{\sqrt{f_2} + \sqrt{f_3}} \tag{20}$$

Eq. (20) is the same as Eq. (13) except that $\sqrt{f}$ replaces f. The reorganization energies of the two reactants are identical, i.e. $\Delta G_2^{cp} = \Delta G_3^{cp}$, and the inner-shell reorganization energy is given by

$$\Delta G_{cp} = \frac{6 f_2 f_3 (\Delta d^0)^2}{(\sqrt{f_2} + \sqrt{f_3})^2} \tag{21}$$

where $2(f_2 + f_3)$ in the denominator of Eq. (14a) has been replaced by $(\sqrt{f_2} + \sqrt{f_3})^2$. The positions of d_{mp} and d_{cp} on the energy surfaces are shown in Figs. 2 and 4 and the various reorganization expressions are summarized in Table 1.

In contrast to homogeneous exchange reactions, only a single redox pair is involved in electron exchange at an electrode. Consequently, in the electrochemical case the energy conservation requirement also defines the minimum reorganization energy and d^* for electron exchange at an electrode is rigorously given by Eq. (20). Thus ΔG^*_{in} is equal to $3 f_2 f_3 (\Delta d^0)^2/(\sqrt{f_2} + \sqrt{f_3})^2$ for the $Fe(H_2O)_6^{2+} - Fe(H_2O)_6^{3+}$ exchange at an electrode, i.e. one-half ΔG_{cp} calculated from Eq. (21) for the homogeneous self-exchange reaction. The same relationship between the homogeneous and electrochemical reorganization energies obtains if a common reduced force constant is used for the individual reactants and products [15].

The contributions of the individual reactants to the reorganization energy are illustrated in Fig. 4 for the case where the force constants of the two reactants differ by a factor of two. Although ΔG^*_{in} and ΔG_{cp} are similar, the contributions of the individual reactants are quite sensitive to the model used. Fig. 5 shows the difference between ΔG^*_{in}, ΔG_{mp} and ΔG_{cp} as a function of f_2/f_3. It is apparent that ΔG_{cp} is close to ΔG^*_{in} for $f_2/f_3 > 0.5$. Moreover, ΔG^*_{in}, ΔG_{mp} and ΔG_{cp} are equal when $f_2/f_3 = 1$, where $d^* = d_{mp} = d_{cp}$. Note that ΔG^*_{in}, ΔG_{mp} and ΔG_{cp} as well as d^*, d_{mp} and d_{cp} become increasingly different when $f_2 \ll f_3$.

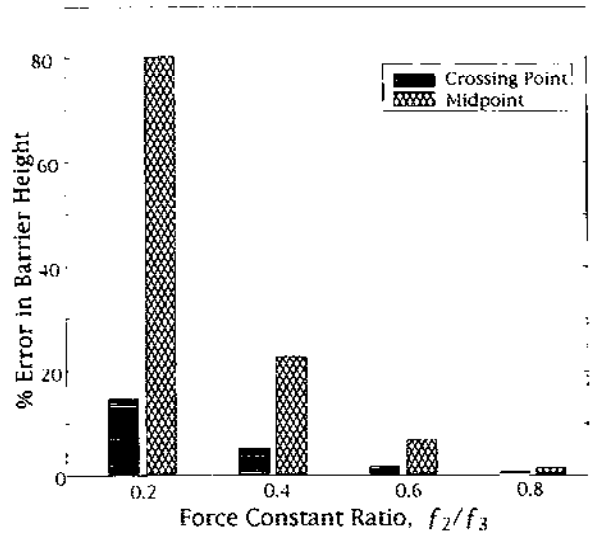

Fig. 5. Bar graph showing the difference between ΔG^*, the inner-shell activation energy given by Eq. (14a), and either ΔG_{cp}, the inner-shell energy required to reach the configuration crossing point shown in Fig. 4 and given by Eq. (21), or ΔG_{mp}, the inner-shell energy required to reach the midpoint configuration shown in Fig. 4 and given by Eq. (19).

Table 1
Energy differences for different values of the reaction coordinate

	Coordinate	Activation energy	Vertical reorganization energy
Transition state	$d^* = \frac{f_2 d_2^o + f_3 d_3^o}{f_2 + f_3}$	$\Delta G_{in}^* = \frac{6 f_2 f_3}{2(f_2 + f_3)} (\Delta d^o)^2$	$3(f_2 + f_3)(\Delta d^o)^2$
Reduced force constant	$d_{in}^* = \frac{1}{2}(d_2^o + d_3^o)$	$\Delta G_{in}^* = \frac{6 f_2 f_3}{2(f_2 + f_3)} (\Delta d^o)^2$	$12 \frac{f_2 f_3}{(f_2 + f_3)} (\Delta d^o)^2$
Midpoint	$d_{mp} = \frac{1}{2}(d_2^o + d_3^o)$	$\Delta G_{mp} = \frac{3(f_2 + f_3)}{4} (\Delta d^o)^2$	$3(f_2 + f_3)(\Delta d^o)^2$
Crossing point	$d_{cp} = \frac{\sqrt{f_2} d_2^o + \sqrt{f_3} d_3^o}{\sqrt{f_2} + \sqrt{f_3}}$	$\Delta G_{cp} = \frac{6 f_2 f_3}{(\sqrt{f_2} + \sqrt{f_3})^2} (\Delta d^o)^2$	$3(f_2 + f_3)(\Delta d^o)^2$

4. Reactant, product and transition state stabilization; adiabatic expressions

The electron transfer formalisms discussed above assume that the barrier lowering as a consequence of the electronic interaction of the reactants may be neglected. As H_{ab} increases, the reactants and products are stabilized and the splitting at the intersection of the reactant and product curves becomes larger. These factors combine to lower the reorganization energy and ultimately to delocalize the system.

4.1. Symmetrical systems

The splitting at the intersection of the diabatic energy curves for a symmetrical system lowers the barrier by H_{ab} (Fig. 1). Further, as H_{ab} increases, the reactant and product minima move closer together and the minima are lowered by H_{ab}^2/λ relative to the diabatic minima [5]. The minima in a symmetrical double-well system are located at $X = [1 \pm (1 - 4H_{ab}^2/\lambda^2)^{1/2}]/2)$ for $H_{ab} \geq \lambda/2$ and the transition state is at $X = 1/2$. For $H_{ab} \geq \lambda/2$ there is a single minimum at $X = 1/2$. In view of these energy changes the free energy of activation for a self-exchange reaction with appreciable coupling of the reactants is given by

$$\Delta G^* = \lambda/4 - H_{ab} + H_{ab}^2/\lambda \tag{22a}$$

$$= \lambda(1 - 2H_{ab}/\lambda)^2/4 \tag{22b}$$

The second and third terms on the right hand side of Eq. (22a) are due to the lowering of the barrier and the stabilization of the reactants, respectively. Eqs. (22a) and (22b) are valid as long as the system is described by a double well potential, i.e. as long as the system remains valence trapped or localized ($H_{ab} < \lambda/2$). The parallel role of $-2H_{ab}$ and $+\Delta G°$ in Eqs. (22b) and (7b), respectively, is noteworthy.

Three classes of symmetrical systems may be distinguished depending on the magnitude of the electronic coupling of the donor and acceptor sites [16]. In Class I systems the coupling is very weak (dashed line, Fig. 1), either because the sites are far apart or because their interaction is symmetry or spin forbidden. The properties of Class I systems are essentially those of the separate reactants. Activated electron transfer either does not occur at all or it occurs only very slowly (because of its high nonadiabaticity) with $\Delta G^* = \lambda/4$. Class II systems ($0 < H_{ab} < \lambda/2$, solid line, Fig. 1) possess new optical and electronic properties in addition to those of the separate reactants. They remain valence trapped or charge localized: the electron transfers range from nonadiabatic ($H_{ab} < 10\ cm^{-1}$) to strongly adiabatic ($H_{ab} > 200\ cm^{-1}$) with ΔG^* given by Eqs. (22a) and (22b). In Class III systems the interaction of the donor and acceptor sites has become so large that two separate minima are no longer discernible and the lower energy surface features a single well. This is the delocalized case which occurs when $H_{ab} \geq \lambda/2$. The latter condition for delocalization follows readily from the zero barrier limit ($\Delta G^* = 0$) of Eqs. (22a) and (22b).

4.2. Unsymmetrical systems

The above classification also applies to unsymmetrical binuclear systems. As in the case of symmetrical systems, the properties of an unsymmetrical Class I system are essentially those of the separate reactants. Although Class II systems remain valence trapped, sufficiently endergonic reactions exhibit a single minimum. The minimum, however, occurs very close to the noninteracting reactant minimum. Provided that $H_{ab} < (\lambda + \Delta G°)/2$ and $|\Delta G°| < \lambda$, the positions of the reactant and product minima are given by Eqs. (23a) and (23b), the location of the transition state is given by Eq. (23c),

$$X_{\min,R} = \frac{H_{ab}^2}{(\lambda + \Delta G°)^2} \tag{23a}$$

$$X_{\min,P} = 1 - \frac{H_{ab}^2}{(\lambda - \Delta G°)^2} \tag{23b}$$

$$X^* = \frac{(\lambda + \Delta G° - 2H_{ab})}{2(\lambda - 2H_{ab})} \tag{23c}$$

and the free energy of activation is given by Eq. (24a)

$$\Delta G^* = \frac{\lambda}{4} + \frac{\Delta G°}{2} + \frac{(\Delta G°)^2}{4(\lambda - 2H_{ab})} - H_{ab} + \frac{H_{ab}^2}{(\lambda + \Delta G°)} \tag{24a}$$

where $\Delta G°$ is the driving force in the *noninteracting* ($H_{ab} = 0$) system. The driving force corrected for the donor–acceptor interaction, i.e. the actual driving force for the adiabatic reaction, is given by Eq. (24b).

$$\Delta G°_{ad} = \Delta G° \left[1 - \frac{2H_{ab}^2}{(\lambda + \Delta G°)(\lambda - \Delta G°)} \right] \tag{24b}$$

The reorganization parameter modified for electron delocalization is given by Eq. (24c) where the $(1 - 2c_b^2)$ factor, with $c_b^2 = X_{min}$, allows for the reduction in the charge transferred [17].

$$\lambda' = \lambda(1 - 2c_b^2)^2 = \lambda\left(1 - \frac{4H_{ab}^2}{\lambda^2}\right) \tag{24c}$$

Note that the parameter λ' used here corresponds to λ_{mod} introduced earlier [17]. Finally, in order for X_{min} to approach the value of 1/2 characteristic of a Class III system, the electronic interaction in an unsymmetrical system has to be large enough to overcome the free energy difference between the initial and final states. This is difficult to accomplish if $|\Delta G°|$ is large. For example, the minimum for an exergonic reaction is located at $X = 0.4$ when $H_{ab} \geq (\lambda + 5|\Delta G°|)/2$. As above, $\Delta G°$ and λ are defined by the diabatic surfaces.

5. Optical charge transfer

In addition to thermal activation, electron transfer between the donor and acceptor sites can also be effected by the absorption of light. As a consequence, λ and H_{ab} can be obtained from spectroscopic properties.

5.1. Symmetrical systems

The energy of the light-induced charge transfer transition in a symmetrical double-well system is given by Eq. (25) [18,19].

$$\nu_{max} = \lambda \tag{25}$$

The band maximum for a symmetrical localized system is *independent* of H_{ab} and Eq. (25) holds throughout the double well regime [8]. Although the repulsion of the reactant and product curves increases with increasing H_{ab}, this is compensated for by the reactant and product minima moving closer together. The net effect of these changes is that the energy difference at the (adiabatic) reactant or product minimum (ν_{max}) remains equal to λ independent of the coupling. Further insight into the relationship between ν_{max} and λ' can be gained by considering the difference between adiabatic and diabatic energy differences. The adiabatic and diabatic energy differences at a particular nuclear configuration are related by Eq. (26a)

$$(G_e - G_g)^2 = (G_P - G_R)^2 + 4H_{ab}^2 \tag{26a}$$

where G_e and G_g are the energies of the upper (excited) and lower (ground) adiabatic energy surfaces, respectively. The optical transition occurs from X_{min}, the reactant minimum of the adiabatic energy surface. At this minimum, $(G_e - G_g)$ is equal to λ and $(G_P - G_R)$ is equal to $\lambda(1 - 2c_b^2)$. Substitution into Eq. (26a) gives

$$\lambda^2 = [\lambda(1 - 2c_b^2)]^2 + 4H_{ab}^2 \tag{26b}$$

Dividing through by λ and substituting $\nu_{max} = \lambda$ and $\lambda' = \lambda[(1 - 2c_b^2)]^2$ gives Eq. (26c). The latter is equivalent to Eq. (24c).

$$\nu_{max} = \lambda' + 4H_{ab}^2/\lambda \tag{26c}$$

The first term on the right hand side of Eq. (26c) is the contribution to the adiabatic energy difference (transition energy) from the delocalization-modified reactant and solvent reorganization energies and the second term is a further contribution to the adiabatic energy difference from electron delocalization. As noted above, their sum is simply equal to the diabatic energy difference at the diabatic minimum.

5.2. Unsymmetrical systems

The energy of the charge transfer transition in an unsymmetrical double-well system is given by

$$\nu_{\max,R}\left(1+\frac{2H_{ab}}{2}\right)\Delta G^{\circ}(\lambda+\Delta G^{\circ})^{3} \tag{27a}$$

provided that $H_{ab}<(\lambda+\Delta G^{\circ})/2$. In this case terms in H_{ab}^{2} contribute to the transition energy. When the H_{ab}^{2} contribution may be neglected, the energy of the charge transfer transition is given by the familiar Eq. (27b).

$$\nu_{\max,R}=\lambda+\Delta G^{\circ} \tag{27b}$$

The various coordinate and energy expressions discussed above, with terms through H_{ab}^{4} included, are summarized in Table 2.

Using the Mulliken formalism, Hush [18] showed that the electronic coupling element is related to the intensity of the charge transfer transition by

$$H_{ab}=2.06\times10^{-2}(\nu_{max}\varepsilon_{max}\Delta\nu_{1/2})^{1/2}/r_{ab} \tag{28a}$$

where ν_{max} and $\Delta\nu_{1/2}$ are the band maximum and width in wave numbers, r_{ab} is the distance separating the donor and acceptor charge centroids in Ångströms, and the band is Gaussian shaped [8]. The Mulliken–Hush equation has been applied to outer-sphere [20] and, more extensively, to bridged [21–26] systems. It is exact within a two-state model and is applicable to symmetrical and unsymmetrical Class II and Class III systems [8]. Within the constraints of a two-state model, the coupling element for a symmetrical Class III system is also given by Eq. (28b)

$$H_{ab}=\nu_{max}/2 \tag{28b}$$

so that H_{ab} for symmetrical Class III complexes can also be obtained directly from the energy of the optical transition [18]. Note that the optical transition in a Class III complex no longer involves charge transfer: the transition occurs between delocalized molecular orbitals of the symmetrical complex and is not accompanied by a net dipole-moment change.

Eqs. (28a) and (28b) are particular forms of the more general equation [8,27]

$$H_{ab}=\left|\nu_{max}\mu_{ge}/(\mu_{b}-\mu_{a})\right| \tag{29a}$$

$$(\mu_{b}-\mu_{a})=[(\mu_{e}-\mu_{g})^{2}+4(\mu_{ge})^{2}]^{1/2} \tag{29b}$$

In these equations μ_{ge} is the transition dipole moment and $(\mu_{b}-\mu_{a})$ is the difference between the dipole moments of the localized initial and final states. The latter dipole-moment difference is related to the measured dipole-moment change $(\mu_{e}-\mu_{g})$ by Eq. (29b) [28]. Eq. (28a) follows from Eq. (29a) by noting that $r_{ab}\equiv\left|(\mu_{b}-\mu_{a})/e\right|$ and that the transition dipole moment is given by Eqs. (30a) and (30b)

$$\mu_{ge}=[f_{os}/(1.08\times10^{-5}\nu_{max})]^{1/2} \tag{30a}$$

$$f_{os}=4.61\times10^{-9}\varepsilon_{max}\Delta\nu_{1/2} \tag{30b}$$

where f_{os} is the oscillator strength for the transition [8,27]. Eq. (28b) is obtained by noting that $(\mu_{e}-\mu_{g})$ is zero for a delocalized system and therefore, from Eq. (29b), $(\mu_{b}-\mu_{a})=2\mu_{ge}$. The relevant dipole-moment changes can be obtained from electroabsorption (Stark) spectroscopy and Eq. (29b) [27].

Table 2
Coordinates and energy expressions[a] for Class I and Class II systems

	Class I	Class II	
	Diabatic $H_{ab}=0$	Symmetric adiabatic $\Delta G^\circ=0$, $H_{ab}<\lambda/2$	Unsymmetric adiabatic[b] $\lvert\Delta G^\circ\rvert<\lambda$, $H_{ab}<(\lambda+\Delta G^\circ)/2$
Reactant minimum, $X_{min,R}$	0	$\frac{1}{2}\left[1-\sqrt{1-\frac{4H_{ab}^2}{\lambda^2}}\right]$	$\frac{H_{ab}^2}{(\lambda+\Delta G^\circ)^2}+\frac{H_{ab}^4(\lambda-3\,\Delta G^\circ)}{(\lambda+\Delta G^\circ)^5}$
Product minimum, $X_{min,P}$	1	$\frac{1}{2}\left[1+\sqrt{1-\frac{4H_{ab}^2}{\lambda^2}}\right]$	$1-\frac{H_{ab}^2}{(\lambda-\Delta G^\circ)^2}+\frac{H_{ab}^4(\lambda+3\,\Delta G^\circ)}{(\lambda-\Delta G^\circ)^5}$
Transition state, X^*	$\frac{\lambda+\Delta G^\circ}{2\lambda}$	1/2	$\frac{(\lambda+\Delta G^\circ-2H_{ab})}{2(\lambda-2H_{ab})}$
Upper surface minimum, $X_{min,e}$	$\frac{\lambda+\Delta G^\circ}{2\lambda}$	1/2	$\frac{(\lambda+\Delta G^\circ+2H_{ab})}{2(\lambda+2H_{ab})}$
Reactant energy[a,c] at $X_{min,R}$	0	$-\frac{H_{ab}^2}{\lambda}$	$-\frac{H_{ab}^2}{(\lambda+\Delta G^\circ)}+\frac{H_{ab}^4\,\Delta G^\circ}{(\lambda+\Delta G^\circ)^4}$
Product energy[a,c] at $X_{min,R}$	$\lambda+\Delta G^\circ$	$\lambda-\frac{H_{ab}^2}{\lambda}$	$(\lambda+\Delta G^\circ)\left[1-\frac{H_{ab}^2(\lambda-\Delta G^\circ)}{(\lambda+\Delta G^\circ)^3}-\frac{H_{ab}^4\,\Delta G^\circ(7\lambda-\Delta G^\circ)}{(\lambda+\Delta G^\circ)^6}\right]$
Splitting at intersection[d]	0	$2H_{ab}$	$2H_{ab}$
Transition state energy[a,c]	$\frac{(\lambda+\Delta G^\circ)^2}{4\lambda}$	$\frac{\lambda}{4}-H_{ab}$	$\frac{(\lambda+\Delta G^\circ)^2}{4\lambda}-H_{ab}+\frac{H_{ab}(\Delta G^\circ)^2}{2\lambda(\lambda-2H_{ab})}$
Activation free energy, ΔG^*	$\frac{(\lambda+\Delta G^\circ)^2}{4\lambda}$	$\frac{(\lambda-2H_{ab})^2}{4\lambda}$	$\frac{\lambda}{4}+\frac{\Delta G^\circ}{2}+\frac{(\Delta G^\circ)^2}{4(\lambda-2H_{ab})}-H_{ab}+\frac{H_{ab}^2}{(\lambda+\Delta G^\circ)}-\frac{H_{ab}^4\,\Delta G^\circ}{(\lambda+\Delta G^\circ)^4}$

Table 2 (*Continued*)

	Class I	Class II	
	Diabatic $H_{ab} = 0$	Symmetric adiabatic $\Delta G° = 0$, $H_{ab} < \lambda/2$	Unsymmetric adiabatic[b] $\lvert\Delta G°\rvert < \lambda$, $H_{ab} < (\lambda + \Delta G°)/2$
Optical transition energy[f], $\nu_{max,R}$	$\lambda + \Delta G°$	λ	$(\lambda+\Delta G°)\left[1+\frac{2H_{ab}^2\ \Delta G°}{(\lambda+\Delta G°)^3}+\frac{2H_{ab}^4\ \Delta G°(3\lambda-\Delta G°)}{(\lambda+\Delta G°)^6}\right]$
Adiabatic free energy change, $\Delta G°_{ad}$	$\Delta G°$	0	$\Delta G°\left[1-\frac{2H_{ab}^2}{(\lambda+\Delta G°)(\lambda-\Delta G°)}-\frac{2H_{ab}^4[\lambda^4+6\lambda^2(\Delta G°)^2+(\Delta G°)^4}{[(\lambda+\Delta G°)(\lambda-\Delta G°)]^4}\right]$
Modified reorganization parameter, λ'	λ	$\lambda-\frac{4H_{ab}^2}{\lambda}$	$\lambda-\frac{4H_{ab}^2}{\lambda}$

[a] The energy scale is set to zero at the energy minimum of the diabatic ($H_{ab} = 0$) reactant curve. $\Delta G°$ is the free energy change between the initial and final diabatic states.

[b] The expressions were derived by using a series expansion to simplify certain expressions. The expressions are only valid in the double minimum regime. If either H_{ab} or $|\Delta G°|$ becomes too large the system develops a single minimum and the equations are no longer valid. The restrictions given in the Table only approximate these conditions due to the complexity of the interaction between H_{ab}, $\Delta G°$ and λ. Note that the H_{ab}^4 terms only contribute when the surface for an exergonic reaction is close to a single minimum.

[c] Note that the minima shift both vertically and horizontally.

[d] The splitting is the vertical separation of the adiabatic curves at $X = (\lambda + \Delta G°)/2\lambda$, the crossing point of the diabatic curves. Note that when $\Delta G° \neq 0$ and $H_{ab} \neq 0$, the transition state and the minimum in the upper curve shift horizontally (in opposite directions) relative to the crossing point of the diabatic surfaces.

[e] Energy of the reactant at the transition state X^*.

[f] The expressions are valid even for endergonic reactions with $\Delta G° > \lambda$.

The metal–metal coupling elements in weakly coupled ligand-bridged mixed-valence systems can be related to the corresponding metal–ligand coupling elements using a superexchange formalism. For example, in MMCT transitions in diruthenium decaammine systems in which the Ru–Ru coupling is provided by mixing with an MLCT state, H_{MM} is given by Eqs. (31a) and (31b) where H_{ML} is the metal–ligand coupling element for $(NH_3)_5Ru^{II}L$ at the Ru^{II}–N equilibrium configuration, $H_{M'L}$ is the corresponding quantity for a $(NH_3)_5Ru^{II}L$ at the Ru^{III}–N geometry, and ΔE_{ML} is the effective metal–ligand energy gap [8].

$$H_{MM} = \frac{H_{ML}H_{M'L}}{2\,\Delta E_{ML}} \tag{31a}$$

$$\frac{1}{\Delta E_{ML}} = \frac{1}{2}\left(\frac{1}{\Delta E_{MLCT}} - \frac{1}{\Delta E_{MLCT} - \Delta E_{MMCT}}\right) \tag{31b}$$

Recent calculations have shown that H_{ML} and $H_{M'L}$ for $(NH_3)_5Ru^{II}L$ complexes do not differ significantly [29]. Indeed, the value of the metal–metal coupling element for $[(NH_3)_5Ru^{II}$–4,4′-bpy-$Ru^{III}(NH_3)_5]^{5+}$, calculated from Eqs. (31a) and (31b) with $H_{ML} = H_{M'L}$, is in satisfactory agreement with the value calculated from the MMCT parameters using Eq. (28a) [17].

6. Comproportionation equilibria

The electronic interaction is an important parameter determining the stability of the binuclear complex formed in a comproportionation reaction [23–25,30]. The comproportionation reaction for a Class II system is

$$\text{II–II} + \text{III–III} = 2(\text{II–III}) \tag{32a}$$

while the corresponding reaction for a Class III system is

$$\text{II–II} + \text{III–III} = 2(\text{III/2–III/2}) \tag{32b}$$

The comproportionation constant K_c and the free energy change for the comproportionation ΔG_c° are conveniently calculated from the difference in the III/II reduction potentials of the oxidized complexes

$$\text{III–III} + e^- = \text{II–III (or III/2–III/2)} \quad E_1^\circ \tag{33a}$$

$$\text{II–III (or III/2–III/2)} + e^- = \text{II–II} \quad E_2^\circ \tag{33b}$$

$$K_c = \exp(\Delta E_c^\circ F/RT) \tag{34a}$$

$$\Delta G_c^\circ = -\Delta E_c^\circ F \tag{34b}$$

In these expressions $\Delta E_c^\circ = (E_1^\circ - E_2^\circ)$, F is the Faraday constant and $\log(K_c) = 16.9\Delta E_c^\circ$ at 25°C where E° is in volts. Since electron delocalization stabilizes the mixed-valence form relative to both the II–II and the III–III forms, ΔE_c° is generally positive. The relationship between ΔE_c° and the width of the intervalence band in symmetrical and unsymmetrical binuclear systems has previously been

considered [31]. Here we consider the connection between ΔE_c° and the energy and intensity of the optical transition in a symmetrical system.

In order to explicitly consider the stabilization of the binuclear complex by the II–III electronic interaction, we break the comproportionation equilibrium into two reactions

$$\text{II–II} + \text{III–III} = 2(\text{II–III})_0 \quad K_{nr},\ \Delta G_{nr}^\circ \tag{35a}$$

$$2(\text{II–III})_0 = 2(\text{II–III}) \text{ (or } 2(\text{III}/2\text{–III}/2)) \quad K_r,\ \Delta G_r^\circ \tag{35b}$$

$$\Delta G_c^\circ = \Delta G_{nr}^\circ + \Delta G_r^\circ \tag{36}$$

where $(\text{II–III})_0$ represents the zero-interaction (charge localized) mixed-valence complex. ΔG_{nr}° includes all the nonresonance contributions to the overall free energy change, namely: a statistical factor of 4, electrostatic interactions (which favor $2(\text{II–III})_0$ relative to $(\text{II–II} + \text{III–III})$), metal–ligand backbonding (which affects the stability of both II–II and II–III), etc. These contributions are generally small. ΔG_r° is the stabilization of *two moles* of the Class II or III complex by the II–III electronic interaction (delocalization) [24,25]. The stabilization of one mole of a symmetrical Class II complex by the II–III electronic interaction is equal to H_{ab}^2/λ (see the discussion leading to Eq. (22a) and Table 2), so that ΔG_r° for a symmetrical Class II complex is twice this value (Eqs. (37a) and (37b)).

$$-\Delta G_r^\circ = 2H_{ab}^2/\lambda \tag{37a}$$

$$= 2H_{ab}^2/\nu_{max} \tag{37b}$$

The resonance stabilization of a symmetrical Class III complex is similarly equal to the difference between the energies of two moles of the fully delocalized complex and of the noninteracting II–III complex.

$$-\Delta G_r^\circ = 2(H_{ab} - \lambda/4) \tag{38a}$$

$$= \nu_{max} - \lambda/2 \tag{38b}$$

In these expressions ν_{max} is the energy of the donor-to-acceptor charge transfer transition in a Class II complex or the energy of the transition between the relevant delocalized molecular orbitals of a Class III complex. Evidently $-\Delta G_r^\circ \approx \nu_{max}/2$ for borderline Class III systems ($H_{ab} \approx \lambda/2$), while $-\Delta G_r^\circ \rightarrow \nu_{max}$ for very strongly coupled systems ($H_{ab} \gg \lambda/2$). For binuclear Ru(II)–Ru(III) systems with predominantly ammine ligands it has been estimated that $\Delta G_{nr}^\circ \approx -500\ \text{cm}^{-1}$, corresponding to $K_{nr} \approx 10$ [24,25,32]. Thus, when $K_c > 10^3$ ($\Delta E_c^\circ > 180$ mV), the comproportionation constant is largely determined by the II–III electronic interaction, i.e. $\Delta G_r^\circ \approx \Delta G_c^\circ = -\Delta E_c^\circ F$. If the interaction becomes sufficiently strong the system will exhibit Class III behavior. Provided all other factors are favorable, Class III behavior is expected for a polyyne-bridged system of reasonable length [33]. For example, comparison of $\Delta E_c^\circ F$ (0.72 eV) and ν_{max} (0.94 eV) for a butadiyne-bridged diferrocene derivative is consistent with the two iron centers being strongly coupled and the system exhibiting intermediate to strong Class III behavior [34].

7. Conclusions

Parabolic energy surfaces for the reactants and products of a self-exchange reaction provide a very good description of the inner-shell reorganization process even when the stretching force constants for the oxidized and reduced forms of the redox couple differ by a factor two. Further, the intersection of the energy parabolas for the oxidized and reduced forms of the couple also provides a good estimate of the reorganization barrier. Although the activation energy is not very dependent on the reorganization criterion, the contributions of the individual reactants to the inner-shell barrier are quite sensitive to the model used.

The comproportionation constant for Class III systems can be related to the energy of the characteristic optical transition. Provided that the binuclear complexes are symmetrical and that the resonance interaction provides the dominant contribution to the comproportionation free energy, $\Delta E_c^\circ \approx \nu_{max}/2$ for borderline Class III systems and $\Delta E_c^\circ \approx \nu_{max}$ for well defined Class III complexes.

Acknowledgements

This research was carried out at Brookhaven National Laboratory under contract DE-AC02-98CH10886 with the US Department of Energy and supported by its Division of Chemical Sciences, Office of Basic Energy Sciences.

References

[1] R.A. Marcus, J. Chem. Phys. 26 (1957) 867.
[2] R.A. Marcus, Discuss. Faraday. Soc. 29 (1960) 21.
[3] R.A. Marcus, N. Sutin, Comments Inorg. Chem. 5 (1986) 119.
[4] R.A. Marcus, Rev. Mod. Phys. 65 (1993) 599.
[5] N. Sutin, Prog. Inorg. Chem. 30 (1983) 441.
[6] J.-K. Hwang, A. Warshel, J. Am. Chem. Soc. 109 (1987) 715.
[7] G. King, A. Warshel, J. Chem. Phys. 93 (1990) 8682.
[8] C. Creutz, M.D. Newton, N. Sutin, J. Photochem. Photobiol. A: Chem. 82 (1994) 4.
[9] N. Sutin, in: G.L. Gunther (Ed.), Bioinorganic Chemistry, vol. 2, Elsevier, New York, 1973, pp. 611–653.
[10] B.S. Brunschwig, J. Logan, M.D. Newton, N. Sutin, J. Am. Chem. Soc. 102 (1980) 5798.
[11] R.A. Marcus, Annu. Rev. Phys. Chem. 15 (1964) 155.
[12] A.B. Myers, Chem. Rev. 96 (1996) 911.
[13] B.S. Brunschwig, S. Ehrenson, N. Sutin, J. Phys. Chem. 90 (1986) 3657.
[14] N. Sutin, C. Creutz, J. Chem. Educ. 60 (1983) 809.
[15] R.A. Marcus, J. Phys. Chem. 67 (1963) 853.
[16] M.B. Robin, P. Day, Adv. Inorg. Chem. Radiochem. 10 (1967) 247.
[17] B.S. Brunschwig, C. Creutz, N. Sutin, Coord. Chem. Rev. 177 (1998) 61.
[18] N.S. Hush, Prog. Inorg. Chem. 8 (1967) 391.
[19] N.S. Hush, Electrochim. Acta 13 (1968) 1005.
[20] J.C. Curtis, T.J. Meyer, Inorg. Chem. 21 (1982) 1562.
[21] D.E. Richardson, H. Taube, J. Am. Chem. Soc. 105 (1983) 40.

[22] C. Creutz, H. Taube, J. Am. Chem. Soc. 95 (1973) 1086.
[23] J.E. Sutton, H. Taube, Inorg. Chem. 20 (1981) 3125.
[24] J.E. Sutton, P.M. Sutton, H. Taube, Inorg. Chem. 18 (1979) 1017.
[25] C. Creutz, Prog. Inorg. Chem. 30 (1983) 1.
[26] R.J. Crutchley, Adv. Inorg. Chem. 41 (1994) 273.
[27] Y.-g. K. Shin, B.S. Brunschwig, C. Creutz, N. Sutin, J. Phys. Chem. 100 (1996) 8157.
[28] R.J. Cave, M.D. Newton, Chem. Phys. Lett. 249 (1996) 15.
[29] Y.-g. Shin, D.J. Szalda, B.S. Brunschwig, C. Creutz, N. Sutin, Inorg. Chem. 36 (1997) 3190.
[30] D.E. Richardson, H. Taube, Coord. Chem. Rev. 60 (1984) 107.
[31] F. Salaymeh, S. Berhane, R. Yusof, R. de la Rosa, E.Y. Fung, R. Matamoros, K.W. Lau, Q. Zheng, E.M. Kober, J.C. Curtis, Inorg. Chem. 32 (1993) 3895.
[32] A.R. Rezvani, C. Bensimon, B. Cromp, C. Reber, J.E. Greedan, V.V. Kondratiev, R.J. Crutchley, Inorg. Chem. 36 (1997) 3322.
[33] N. Sutin, in: J.R. Bolton, N. Mataga, G. McLendon (Eds.), Electron Transfer in Inorganic, Organic, and Biological Systems, Advances in Chemistry 228, American Chemical Society, Washington, DC, 1991, pp. 25–43.
[34] N. Le Narvor, L. Toupet, C. Lapinte, J. Am. Chem. Soc. 117 (1995) 7129.